Anesthetics Alter the Physical and Functional Properties of the Ca-ATPase in Cardiac Sarcoplasmic Reticulum

Brad S. Karon,* Lisa M. Geddis,‡ Howard Kutchai,‡ and David D. Thomas*

*Department of Biochemistry, University of Minnesota Medical School, Minneapolis, MN 55455, and ‡Department of Molecular Physiology and Biological Physics, University of Virginia, Charlottesville, VA 22908, USA

ABSTRACT We have studied the effects of the local anesthetic lidocaine, and the general anesthetic halothane, on the function and oligomeric state of the Ca-ATPase in cardiac sarcoplasmic reticulum (SR). Oligomeric changes were detected by time-resolved phosphorescence anisotropy (TPA). Lidocaine inhibited and aggregated the Ca-ATPase in cardiac SR. Micromolar calcium or 0.5 M lithium chloride protected against lidocaine-induced inhibition, indicating that electrostatic interactions are essential to lidocaine inhibition of the Ca-ATPase. The phospholamban (PLB) antibody 2D12, which mimics PLB phosphorylation, had no effect on lidocaine inhibition of the Ca-ATPase in cardiac SR. Inhibition and aggregation of the Ca-ATPase in cardiac SR occurred at lower concentrations of lidocaine than necessary to inhibit and aggregate the Ca-ATPase in skeletal SR, suggesting that the cardiac isoform of the enzyme has a higher affinity for lidocaine. Halothane inhibited and aggregated the Ca-ATPase in cardiac SR. Both inhibition and aggregation of the Ca-ATPase by halothane were much greater in the presence of PLB antibody or when PLB was phosphorylated, indicating a protective effect of PLB on halothane-induced inhibition and aggregation. The effects of halothane on cardiac SR are opposite from the effects of halothane observed in skeletal SR, where halothane activates and dissociates the Ca-ATPase. These results underscore the crucial role of protein-protein interactions on Ca-ATPase regulation and anesthetic perturbation of cardiac SR.

INTRODUCTION

The Ca-ATPase of SR pumps Ca from the sarcoplasm into the SR lumen to allow relaxation of both skeletal and cardiac muscle. Previous investigations into the regulatory mechanisms of the SR Ca-ATPase in skeletal muscle have established the importance of the Ca-ATPase oligomeric state to enzymatic function (Squier et al., 1988b; Voss et al., 1991; Karon and Thomas, 1993). Agents that aggregate the Ca-ATPase in skeletal SR, such as chemical cross-linkers, the amphipathic peptide melittin, or the local anesthetic lidocaine, inhibit enzymatic activity (Squier et al., 1988b; Mahaney and Thomas, 1991; Voss et al., 1991; Kutchai et al., 1994). Agents that dissociate the Ca-ATPase, such as the volatile anesthetics ether and halothane, activate the enzyme (Bigelow and Thomas, 1987: Birmachu et al., 1989; Karon and Thomas, 1993).

In cardiac SR, the integral membrane protein PLB regulates the enzymatic activity of the Ca-ATPase (Lindemann et al., 1983). At submicromolar levels of Ca, PLB-ATPase interaction results in an inhibition of enzymatic activity (James et al., 1989; Sham et al., 1991). PLB-ATPase interaction (at submicromolar Ca) also results in decreased Ca-ATPase rotational mobility (compared with high Ca or PLB phosphorylation) (Voss et al., 1994). Upon PLB phosphorylation or addition of micromolar Ca, the resting inhibition of the Ca-ATPase is relieved (the enzyme is activated). This activation correlates with an increase in the rotational mobility of the Ca-ATPase, most likely because the physical interaction between PLB and the Ca-ATPase is disrupted, allowing large Ca-ATPase oligomers to dissociate (Voss et al., 1994). The physical and biochemical mechanisms by which PLB regulates Ca-ATPase function are just beginning to be elucidated.

Local anesthetics, such as lidocaine, have been reported to inhibit the Ca-ATPase in cardiac SR (Katz et al., 1975). Lidocaine also acts as an anti-arrhythmic agent in the heart, although the concentrations of lidocaine necessary to inhibit the Ca-ATPase are far greater than effective anti-arrhythmic levels (Katz et al., 1975). In skeletal muscle, cationic agents similar to lidocaine have been found to inhibit the Ca-ATPase in a manner analogous to the action of PLB in cardiac SR (Mahaney and Thomas, 1991; Hughes et al., 1994). In addition, lidocaine induces the formation of larger Ca-ATPase oligomers in skeletal SR (Kutchai et al., 1994), similar to the effects of unphosphorylated PLB in cardiac SR. Therefore, studying lidocaine's effect in cardiac SR may not only provide more information on the effects of anti-arrhythmic agents on the heart but also provide information about the regulation of the Ca-ATPase by PLB.

Volatile anesthetics, such as halothane, are known to depress myocardial contractility at clinical levels, and this effect may be due to a defect in SR Ca regulation (Rusy and Komai, 1987). Thus, an understanding of halothane action on the Ca-ATPase in cardiac SR is crucial to understanding the

Received for publication 12 September 1994 and in final form 16 November 1994.

Address reprint requests to Dr. David D. Thomas, Department of Biochemistry, University of Minnesota Medical School, Millard 4–225, 435 Delaware Street, SE, Minneapolis, MN 55455. Tel.: 612-625-0957; Fax: 612-624-0632; E-mail: ddt[com@]ddt.biochem.umn.edu.

Abbreviations used: SR, sarcoplasmic reticulum; PLB, phospholamban; Ab, antibody; ERITC, erythrosin-5-isothiocyanate; DMF, *N,N*-dimethylformamide; MOPS, 3-(*N*-morpholino)propanesulfonic acid; CSR, cardiac sarcoplasmic reticulum; EGTA, ethyleneglycol-*bis*-(β-aminoethyl ether)-*N,N,N′,N′*-tetra-acetic acid; TPA, time-resolved phosphorescence anisotropy; NADH, β-nicotinamide adenine dinucleotide, reduced form.

0006-3495/95/03/936/10 $2.00

action of anesthetics on the heart. Previous studies of the effects of anesthetics in cardiac SR have reached different conclusions, finding either activation or inhibition of the Ca-ATPase by halothane (Lain et al., 1968; Casella et al., 1987; Frazer and Lynch, 1992). It was previously observed that halothane dissociates Ca-ATPase oligomers in skeletal SR, correlating with activation of the Ca-ATPase (Karon and Thomas, 1993; Karon et al., 1994).

Because it has been established in skeletal SR that anesthetic-induced activation (inhibition) correlates well with anesthetic-induced dissociation (aggregation) of the Ca-ATPase (Thomas and Karon, 1994), it is important to study not only functional but also physical effects of anesthetics in cardiac SR. However, none of the studies on lidocaine or halothane action in cardiac SR has considered the effects of these anesthetic agents on the oligomeric state of the Ca-ATPase. Moreover, because PLB regulation of the Ca-ATPase also involves changes in oligomeric state (Voss et al., 1994), the role of PLB in mediating anesthetic effects on Ca-ATPase function and oligomeric state must be considered. In the present study, to gain a more complete understanding of anesthetic action in the heart, we have studied the effects of halothane and lidocaine (as mediated by PLB) on Ca-ATPase oligomeric state, as detected by time-resolved phosphorescence anisotropy (TPA), and enzymatic function in cardiac SR.

MATERIALS AND METHODS

Reagents and solutions

ERITC was obtained from Molecular Probes (Eugene, OR) and stored in DMF under liquid nitrogen. Halothane (99%) was obtained from Aldrich (Milwaukee, WI). Lidocaine, catalase, glucose oxidase, β-D-glucose, pyruvate kinase, lactate dehydrogenase, phosphoenol pyruvate, ATP, and NADH were purchased from Sigma Chemical Co. (St. Louis, MO). The calcium ionophore A23187 was obtained from Calbiochem (San Diego, CA). ATPase assays and spectroscopic measurements were carried out at 25°C in a standard buffer containing 50 mM MOPS (pH 7), 60 mM KCl, 2 mM $MgCl_2$, and either $CaCl_2$ alone or 5 mM EGTA + $CaCl_2$ to reach the desired concentration of free Ca. Unless otherwise indicated, [Ca] will be used to indicate the concentration of free ionized Ca^{2+}, calculated as described previously (Voss et al., 1994).

Preparations and assays

CSR vesicles prepared from canine ventricular tissue were kindly provided by Dr. Joseph J. Feher (Feher and Briggs, 1983). Ca-ATPase activity was assayed by an enzyme-linked, continuous assay (Karon et al., 1994). Between 5 and 50 μg/ml of Ca-ATPase in SR vesicles was added to a buffer containing 2 mM phosphoenol pyruvate, 0.24 mM NADH, 120 IU of pyruvate kinase, and 120 IU of lactate dehydrogenase. The assay mixture also contained 1 μg/ml of the ionophore A23187 (in DMF) to prevent a buildup of calcium inside the vesicles that might inhibit the Ca-ATPase activity. Lidocaine (in 50% ethanol) and halothane (in DMF) were added to the samples and allowed to incubate for 5 min before data collection. The volume of ethanol or DMF added (<1% v/v) to the sample did not affect Ca-ATPase activity. Halothane was added as described previously (Karon and Thomas, 1993), such that partitioning of halothane into the vapor phase was negligible. MgATP (1 mM) was added to start the assay, and the absorbance of NADH was followed at 340 nm to determine the amount of ATP hydrolyzed. The monoclonal anti-PLB Ab 2D12 was provided by Dr. Larry Jones (Cantilina et al., 1993), and activity experiments in the presence of PLB Ab were performed by incubating Ab (1:2 Ab:Ca-ATPase by weight) at 25°C for 20 min before the start of the assay. Ca uptake measurements were obtained as described previously (Kutchai and Campbell, 1989) in the presence of 50 mM MOPS, 70 mM KCl, 0.5 mM EGTA, 5 mM potassium oxalate, 5 mM sodium azide, 0.383 mM $CaCl_2$ (free [Ca] = 1 μM), 1 μCi ^{45}Ca/ml, and 3 mM MgATP, with and without 1 μM ruthenium red and 0–30 mM lidocaine. For Ca-ATPase activity and TPA experiments, PLB was specifically phosphorylated in CSR as described previously (Voss et al., 1994).

Phosphorescence experiments

The Ca-ATPase was specifically labeled at lysine 515 with ERITC as described previously (Birmachu and Thomas, 1990). After labeling, samples were diluted to a concentration of 0.2–0.3 mg/ml in the standard buffer. Oxygen was removed from the sample by the addition of 200 μg/ml glucose oxidase, 30 μg/ml catalase, and 5 mg/ml β-D-glucose (Eads et al., 1984). Deoxygenation was allowed to proceed for 20 min before data collection. Lidocaine and halothane were added in a manner analogous to that used for ATPase activity experiments and allowed to incubate 5–10 min before data collection. Neither halothane, lidocaine, nor oxygen that may have entered the sample upon addition of anesthetics was found to measurably change the probe luminescence lifetime.

The anisotropy is defined as

$$r(t) = \frac{I_{vv} - GI_{vh}}{I_{vv} + 2GI_{vh}} \quad (1)$$

where I_{vv} and I_{vh} are the vertical and horizontal components of the emission after excitation with a vertically polarized pulse. Time-resolved phosphorescence anisotropy (TPA) decays were recorded with an instrument described previously (Ludescher and Thomas, 1988), by signal averaging the time-dependent phosphorescence decays with a single detector and a polarizer that alternates between vertical ($I_{vv}(t)$) and horizontal ($I_{vh}(t)$) orientation every 2000 laser flashes. G is an instrumental correction factor, determined by measuring the anisotropy of a solution of free dye under experimental conditions and adjusting G to give an anisotropy value of zero, the theoretical value for a freely tumbling chromophore (G generally varies between 0.996–1.004 for our spectrometer).

Data analysis

TPA decays were analyzed by fitting them as described by Mersol et al. (1995), with the nonlinear least squares algorithm of Marquardt (Bevington, 1969). The quality of the fit was gauged by comparing χ^2 values and by evaluating the residuals. Previous reports from this laboratory (Birmachu and Thomas, 1990; Karon et al., 1994; Mersol et al., 1995) have shown that the TPA of ERITC-SR is dominated by the uniaxial rotational diffusion of the labeled Ca-ATPase about an axis normal to the bilayer, and that it is a good approximation to fit a sum of three exponentially decaying terms plus a constant term to the data

$$\frac{r(t)}{r(0)} = \sum_{i=1}^{3} A_i e^{-t/\phi_i} + A_\infty \quad (2)$$

where ϕ_i, the rotational correlation time of the ith component, is inversely proportional to the rotational diffusion coefficient D_i, A_i is proportional to the mole fraction of Ca-ATPase with a correlation time ϕ_i, and A_∞ is the normalized residual anisotropy (r_∞/r_0). The value of A_∞ depends on the orientation of the probe transition dipoles with respect to the membrane normal (see Scheme 1) as well as the fraction of Ca-ATPase molecules immobile on the time scale of the experiment (Cornea and Thomas, 1994; Karon et al., 1994; Mersol et al., 1994). The orientational dependence of A_∞ is described by

$$A_{\infty 0} = \frac{P_2(\cos\theta_a)P_2(\cos\theta_e)}{P_2(\cos\delta)} \quad (3)$$

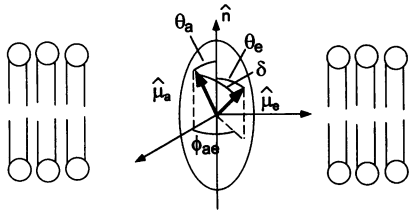

SCHEME 1. An illustration of the angles used in Eqs. 3 and 8. The probe's absorption ($\hat{u}_a$) and emission ($\hat{u}_e$) dipoles are shown relative to the membrane normal. θ_a is the angle between the membrane normal and the probe's absorption dipole, and θ_e is the angle between the membrane normal and the probe's emission dipole. δ is the angle between the probe's absorption and emission dipoles, and ϕ_{ae} is the azimuthal angle between the probe's absorption and emission dipoles.

where $P_2(x) = (3x^2 - 1)/2$, θ_a is the angle between the probe absorption dipole and the membrane normal, θ_e is the angle between the probe emission dipole and the membrane normal, and δ is the angle between the absorption and emission transition dipoles (Lipari & Szabo, 1980). An increase in A_∞ due to an increased fraction of immobile aggregates can be expressed as A'_∞ (Karon and Thomas, 1993)

$$A'_\infty = A_{\infty\,\text{observed}} - A_{\infty\,0} \tag{4}$$

where $A_{\infty\,0} = 0.18$, determined experimentally by measuring the residual anisotropy of the Ca-ATPase in the absence of large aggregates (light skeletal SR at 25°C) (Karon et al., 1994).

In the present study we have also fit the data to the analytical function that Eq. 2 approximates, which incorporates all of the terms that describe the anisotropy of uniaxially rotating chromophores

$$r(t) = \sum_{i=1}^{n} f_i r_i(t) + f_I r_0 \tag{5}$$

where f_i is the mole fraction associated with the ith rotating species, and f_I is the mole fraction of Ca-ATPase not rotating on the time scale of the experiment (immobilized Ca-ATPase). With this expression, changes in the mole fraction of immobile Ca-ATPase induced by SR perturbants can be directly determined, independent of the orientation of the probe (Mersol et al., 1994). Because the probe dipole angles are most likely identical for ERITC-labeled skeletal and cardiac SR (Voss et al., 1994), the value of $A_{\infty\,0}$ (Eq. 3) determined from TPA decays of ERITC-skeletal SR was used to calculate the value of A'_∞ (Eq. 4) for ERITC-CSR samples. A'_∞ is related to the mole fraction of immobilized Ca-ATPase by the following expression (Cornea and Thomas, 1994)

$$f_I = A'_\infty/(1 - A_{\infty 0}). \tag{6}$$

Thus, the value of f_I determined directly by fitting TPA decays to the uniaxial model (Eq. 5) can be compared with the value of f_I calculated by fitting TPA decays to the simple multiexponential model (Eqs. 2–4 and 6).

The expression for the individual anisotropy of the ith uniaxially rotating species is given by (Szabo, 1984)

$$r_i(t) = \kappa\,(a_1 e^{-D_i t} + a_2 e^{-4D_i t} + a_3) \tag{7}$$

with

$$a_1 = \tfrac{6}{5} \sin\theta_a \cos\theta_a \cos\phi_{ae} \cos\theta_e \sin\theta_e \tag{8a}$$

$$a_2 = \tfrac{3}{10} \sin^2\theta_a \sin^2\theta_e \cos 2\phi_{ae} \tag{8b}$$

$$a_3 = \tfrac{1}{10}(3\cos^2\theta_e - 1)(3\cos^2\theta_a - 1). \tag{8c}$$

Here, D_i is the rotational diffusion coefficient about the normal to the membrane, and ϕ_{ae} is the azimuthal angle between the absorption and emission transition dipoles of the probe (see Scheme 1). κ is the order parameter for fast (sub-microsecond) rotation of the probe with respect to the protein and is given in general form by

$$\kappa = \tfrac{1}{2}(3\cos^2\Delta\theta - 1) \tag{9}$$

where $\Delta\theta$ describes the amplitude of the motion. This motion may result from the site of probe attachment (Lys 515) undergoing segmental motion or from partial freedom of motion of the probe itself around the site of attachment. It can be modeled as wobble-in-a-cone type motion, in which the probe is free to move within a cone of half-angle θ_c centered about an axis determined by the probe's local environment. In this case κ is given by (Kinosita et al., 1977)

$$\kappa = [\tfrac{1}{2}\cos\theta_c(1 + \cos\theta_c)]^2. \tag{10}$$

The more complete model (described by Eqs. 5 and 7–10) differs from previous analysis (described by Eqs. 2–4 and 6) only in 1), the inclusion of the bi-exponential decay for each species (Eq. 7); 2), the explicit inclusion of the fast wobble parameter κ (Eqs. 7, 9, and 10); and 3), the explicit inclusion of the angular dependence of the amplitudes of the exponentially decaying terms (Eq. 8, a-c). It has been observed previously that TPA decays of ERITC-SR are best fit by a function that includes three rotating species. Each species is assumed to have the same values of ϕ_{ea}, θ_a, and θ_e and to differ from the other species only in its diffusion coefficient, presumably due to differences in aggregation state (Mersol et al., 1994).

The rotational diffusion coefficient of these rotating species is predicted by the Saffman-Delbrück equation (Saffman and Delbrück, 1975)

$$D = kT/(4\pi a^2 h\eta) \tag{11}$$

where a is the effective radius of the protein in the bilayer, h is the height of the protein in contact with the membrane, k is Boltzmann's constant, η is the effective membrane viscosity, and T is the absolute temperature. Thus, the rotational diffusion coefficient is proportional to the lipid fluidity (T/η) Squier et al., 1988b) and inversely proportional to the intramembrane cross-sectional area (πa^2) of the protein. An increase in lipid fluidity or a decrease in the effective radius of the rotating species will cause an increase in the protein's rotational diffusion coefficient. This has been confirmed by previous studies on the Ca-ATPase using saturation transfer electron paramagnetic resonance (Squier et al., 1988a) and phosphorescence anisotropy (Birmachu and Thomas, 1990). The latter study showed that correlation times (ϕ_i, eq 2) obtained by fitting TPA decays can be used to determine the sizes of Ca-ATPase oligomers, and normalized amplitudes (A_i in Eq. 2 and f_i in Eq. 5) can be used to determine the mole fractions of oligomers present in SR.

RESULTS

Effects of lidocaine on Ca-ATPase activity and uptake in cardiac SR

To determine the effect of lidocaine on the function of the Ca-ATPase in cardiac SR, we measured the rate of Ca-dependent ATP hydrolysis (Ca-ATPase activity) in the presence of 1 μg/ml ionophore A23187 and the rate of Ca uptake by SR vesicles in the absence and presence of 1 μM of the Ca release inhibitor ruthenium red. Ca-ATPase activity and uptake rates measured at 1 μM [Ca] are shown in Fig. 1. Lidocaine inhibited Ca-ATPase activity at 1μM [Ca], and the inhibition of Ca-ATPase activity by lidocaine paralleled the inhibition of Ca uptake by lidocaine in the absence of ruthenium red. In the presence of 1 μM ruthenium red, Ca uptake rates were higher and inhibition of lidocaine steeper than observed in the absence of the Ca release inhibitor. It has previously been determined that ruthenium red (up to 20 μM) does not affect the rate of Ca uptake by the Ca-ATPase and thus most likely increases the coupling ratio (ratio of Ca

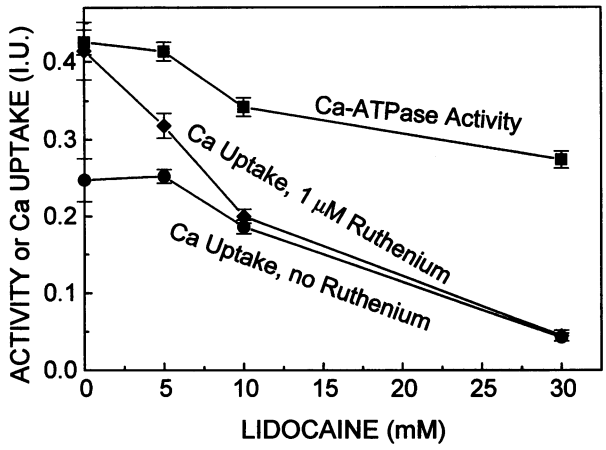

FIGURE 1 Ca-ATPase activity at 25°C and 1 μM [Ca] in the presence of 1 μg/ml of the ionophore A23187 (■); compared with Ca uptake in the absence (●) and presence (♦) of 1 μM ruthenium red at 25°C, as described in Materials and Methods. IU, μmol of ATP hydrolyzed (Ca uptake)/mg SR protein/min. The coupling ratio (ratio of Ca uptake to ATPase activity) is approximately 1 in the presence of ruthenium red, but much less in the absence of ruthenium. Each point represents the average of 2–4 experiments ± SD.

uptake to ATPase activity) by inhibiting Ca release from SR (Moutin et al., 1992). The higher rate of uptake observed suggests that Ca uptake was more tightly coupled to ATP hydrolysis in the presence of ruthenium red but that lidocaine may have had two effects in the presence of ruthenium: (1) inhibition of the Ca-ATPase and (2) uncoupling Ca transport from ATP hydrolysis.

Because it has previously been observed that lidocaine inhibition is partially reversed by Ca (Katz et al., 1975), we determined the effects of lidocaine on the activation of the Ca-ATPase by Ca. In cardiac SR the K_m for Ca has been reported to be 0.2–1.5 μM [Ca] (Sasaki et al., 1992; Cantilina et al., 1993). As shown in Fig. 2, lidocaine had no significant effect on the activation of the Ca-ATPase by Ca in the range of 0–5 μM. We conclude that lidocaine had no effect on the K_m for Ca.

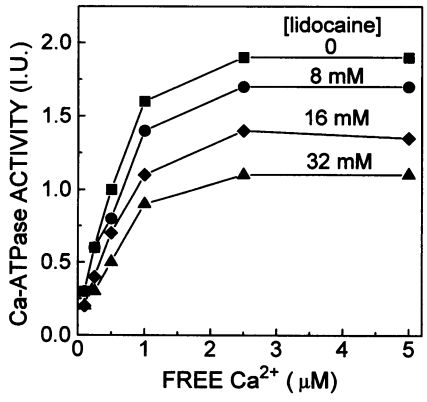

FIGURE 2 Ca-ATPase activity at 25°C between 0 and 5 μM [Ca] in the presence of 0 (■), 8 (●), 16 (♦), and 32 (▲) mM lidocaine, as described in Materials and Methods (IU, μmol of ATP hydrolyzed/mg SR protein/min). Each point represents the average of four experiments.

However, higher Ca levels did have a protective effect against lidocaine inhibition of the Ca-ATPase in cardiac SR. Inhibition of the Ca-ATPase was greatest at 150 nM [Ca], with Ca levels up to 500 μM having a protective effect against lidocaine inhibition (Fig. 3). To determine whether Ca (as a specific substrate) was necessary to protect the Ca-ATPase against lidocaine-induced inhibition, we determined the effect of 0.5 M LiCl in the presence of 20 μM [Ca] on the inhibition of the Ca-ATPase by lidocaine (Fig. 3). This concentration of LiCl was previously shown to protect against Ca-ATPase inhibition by polylysine in skeletal SR, presumably by acting as a nonspecific cation interfering with electrostatic interactions between polylysine and the Ca-ATPase (Voss et al., 1991). In the presence of 0.5 M LiCl, lidocaine between 0 and 30 mM had no effect on Ca-ATPase activity (Fig. 3).

To further define the role of cationic charge in lidocaine-induced inhibition, we measured the effects of the uncharged local anesthetic benzocaine on Ca-ATPase activity and found no inhibition by benzocaine between 0 and 1 mM (not shown). To determine whether the regulatory state of PLB affected lidocaine-induced inhibition of the Ca-ATPase, we added PLB Ab to CSR at 150 nM [Ca] (to remove the inhibitory effects of PLB). Addition of PLB Ab did not change the extent of inhibition of the Ca-ATPase by lidocaine (not shown), suggesting that PLB does not influence lidocaine-induced inhibition of the Ca-ATPase.

Effects of lidocaine on the rotational dynamics of the Ca-ATPase

When lidocaine is added to ERITC-CSR at 100 μM [Ca], it decreases the apparent rate of TPA decay and increases the residual anisotropy (Fig. 4). A slower anisotropy decay may be due to either (1) decreased rotational diffusion of Ca-ATPase oligomers due to decreased lipid fluidity (T/η; Eq. 11), or (2) formation of larger Ca-ATPase oligomers

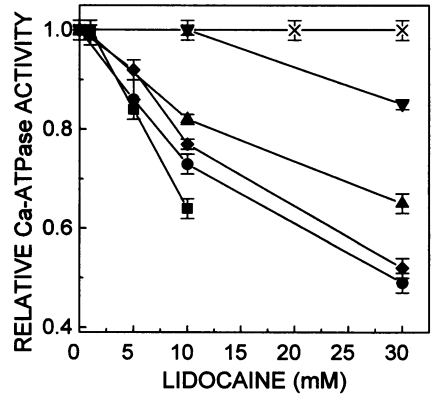

FIGURE 3 Relative Ca-dependent ATPase activity at 25°C (normalized to the Ca-ATPase activity in the absence of lidocaine at each Ca concentration) at 150 nM (■), 1 μM (●), 20 μM (♦), 100 μM (▲), and 500 μM (▼) [Ca] and at 20 μM [Ca] + 0.5 M LiCl (X) in the absence and presence of lidocaine, as described in Materials and Methods. Each point represents the average of three experiments ± SE.

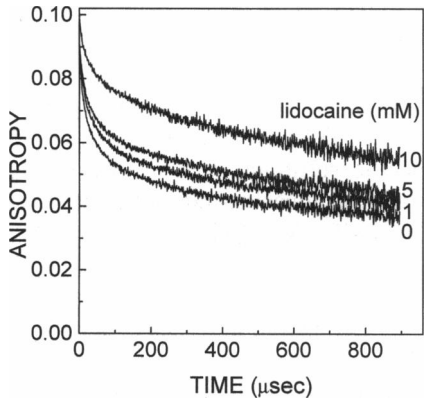

FIGURE 4 TPA decays of ERITC-CSR at 25°C and 100 μM [Ca] in presence of 0, 1, 5, and 10 mM lidocaine.

(increase in a; Eq. 11). It was previously determined that changes in Ca-ATPase oligomeric state and not SR lipid fluidity were responsible for lidocaine-induced increases in the residual anisotropy of ERITC-skeletal SR (Kutchai et al., 1994). Therefore, we conclude that the increase in residual anisotropy induced by lidocaine in ERITC-CSR is due to an increased fraction of immobile Ca-ATPase aggregates (f_i; Eq. 6).

Because lidocaine-induced inhibition of Ca-ATPase activity was dependent upon the concentration of Ca (or LiCl) present, we determined the effects of Ca and 0.5 M LiCl on lidocaine-induced aggregation of the Ca-ATPase. TPA decays of ERITC-CSR in the absence and presence of 5 mM lidocaine at 50 nM, 150 nM, 100 μM, and 500 μM [Ca] are shown in Fig. 5. At 50 and 150 nM [Ca] (Fig. 5*A*), 5 mM lidocaine slowed the rate of TPA decay but did not have an effect on the residual anisotropy. At 500 μM [Ca], 5 mM lidocaine increased the residual anisotropy of ERITC-CSR but not to the extent observed at 100 μM [Ca] (Fig. 5*B*). Addition of 0.5 M LiCl to ERITC-CSR at 100 μM [Ca] did not prevent aggregation (as indicated by an increase in the residual anisotropy) of the Ca-ATPase by 5 mM lidocaine (not shown).

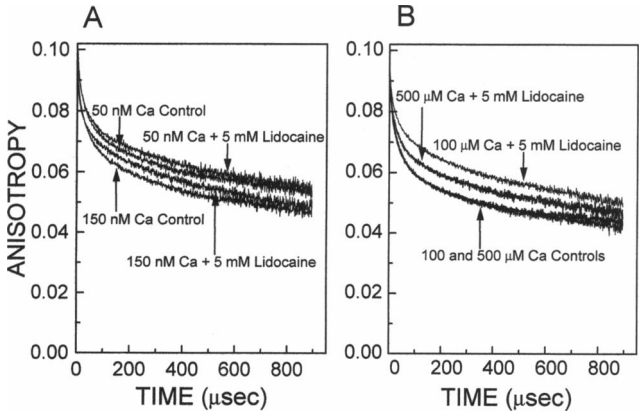

FIGURE 5 TPA decays of ERITC-CSR at 25°C. From bottom to top: 150 nM [Ca], 150 nM [Ca] + 5 mM lidocaine, 50 nM [Ca], and 50 nM [Ca]+ 5 mM lidocaine (*A*) and 100 μM and 500 μM [Ca] controls, 500 μM [Ca] + 5 mM lidocaine, and 100 μM [Ca] + 5 mM lidocaine (*B*).

Effects of halothane on Ca-ATPase activity

We determined the effects of halothane on Ca-ATPase activity at 100 μM [Ca], and at 150 nM [Ca] in the absence and presence of PLB Ab, as well as after PLB phosphorylation (Fig. 6). At 100 μM [Ca], halothane inhibited the Ca-ATPase monotonically. Clinical levels of halothane have been reported to be between 0.25 and 0.4 mM (Rusy and Komai, 1987; Franks and Lieb, 1994); thus, clinical levels of halothane had little effect on the Ca-ATPase at very high levels of Ca (Fig. 6). At subsaturating levels of Ca (150 nM), near clinical levels of halothane activated the Ca-ATPase in CSR. However, when PLB was specifically phosphorylated, or when PLB Ab was added to mimic PLB phosphorylation, these levels of halothane inhibited the Ca-ATPase (Fig. 6).

It has been reported previously that halothane inhibition of the Ca-ATPase in CSR is competitive with respect to Ca (Malinconico and McCarl, 1982). We found that at higher levels of halothane (2–5 mM), inhibition by halothane was more severe at low rather than high Ca concentration indicating a protective effect of Ca on halothane inhibition of the Ca-ATPase (Fig. 6). It has also been reported that inhibition of the Ca-ATPase in CSR is dependent on the concentration of ATP present (Blanck and Thompson, 1981). However, at 100 μM [Ca], ATP concentrations between 20 μM and 5 mM had no effect on the relative inhibition of the Ca-ATPase by 0–5 mM halothane (not shown).

Effects of halothane on the rotational dynamics of the Ca-ATPase

We used TPA to determine the effects of halothane on the Ca-ATPase oligomeric state in CSR. Fig. 7 shows the anisot-

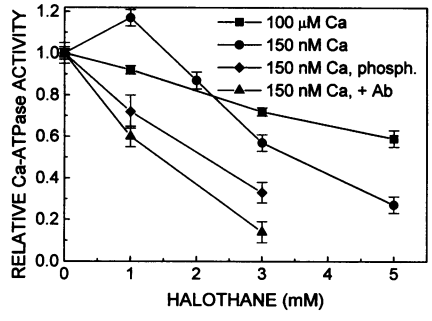

FIGURE 6 Relative Ca-dependent ATPase activity (normalized to the Ca-ATPase activity in the absence of halothane at each Ca concentration) at 25°C and 150 nM [Ca] (●) or 100 μM [Ca] (■), in the absence and presence of halothane. ATPase activity at 150 nM [Ca] after PLB had been specifically phosphorylated (♦) or in the presence of PLB Ab (▲) is also shown. PLB Ab had no effect on ATPase activity at 100 μM [Ca] in the absence or presence of halothane (not shown). ATPase activity (μmol of ATP hydrolyzed/mg SR protein/min) in the absence of halothane was 0.30 ± .01 (150 nM [Ca]), 0.72 ± .04 (150 nM [Ca] + Ab), 0.67 ± .02 (150 nM [Ca], PLB phosphorylated), and 1.23 ± .04 (100 μM [Ca]).

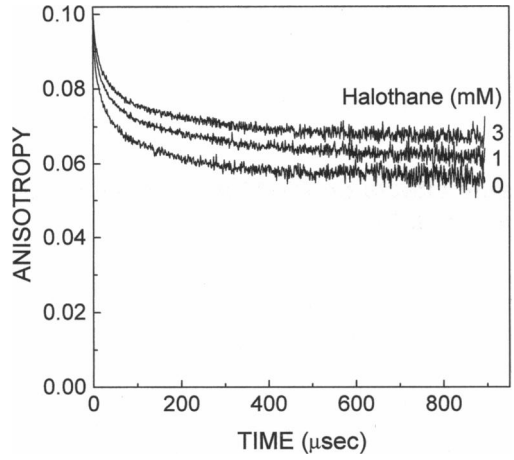

FIGURE 7 TPA decays of ERITC-CSR at 25°C and 50 nM [Ca] after PLB had been specifically phosphorylated, in the absence and presence of halothane.

ropy decays of ERITC-CSR at 50 nM [Ca], after PLB had been specifically phosphorylated, in the presence of 0, 1, and 3 mM halothane. Because halothane increases the fluidity of (rabbit skeletal) SR lipid (Karon and Thomas, 1993), and the lipid composition and fluidity are very similar in rabbit skeletal SR and dog CSR (Birmachu et al., 1993), changes in SR lipid fluidity cannot account for halothane-induced increases in residual anisotropy. Thus, we conclude that halothane increased the fraction of immobile Ca-ATPase aggregates.

We fit the anisotropy decays of ERITC-CSR in the absence and presence of halothane according to two models: (1) a multiexponential decay, in which the mole fraction of immobile aggregates ($f_I = A_\infty'/1 - A_{\infty 0}$) is calculated by measuring an increase in the residual anisotropy above the value measured for SR in the absence of large aggregates ($A_\infty' > A_{\infty 0}$, Eq. 4); and (2) the uniaxial decay model (Eq. 5), in which the mole fraction of immobile aggregates (f_I) is determined directly from parameters of the fit. The mole fraction of immobile aggregates (f_I) determined by the two models shows excellent agreement (Table 1), suggesting that the simple multiexponential fit can be used to obtain information about the mole fraction of immobile Ca-ATPase species in SR. Both models demonstrate that halothane-induced aggregation correlates well with halothane-induced inhibition of the Ca-ATPase (Table 1). Low levels of halothane (1 mM) produced significant effects on the fraction of immobile Ca-ATPase aggregates (f_I) only in the low Ca, PLB-phosphorylated sample. These same conditions produced the greatest extent of Ca-ATPase inhibition at low levels of halothane (Table 1).

The effects of halothane on the angles (Eqs. 3 and 8) between the membrane normal and emission (θ_e) and absorption (θ_a) dipoles, and the submicrosecond motion of the probe on the protein (κ; Eqs. 5, 7, and 8) are plotted in Fig. 8 *A*. Halothane appears to increase the extent of fast probe motion, without changing the angles between the absorption and emission dipoles and the membrane normal. The effects of

TABLE 1 TPA Parameters of ERITC-CSR and enzymatic activity at 0–3 mM halothane

Sample	f_I (uniaxial)	$f_I = \frac{A_\infty'}{1 - A_{\infty 0}}$	% Inhibition
100 μM Ca	0.27	0.29 ± 0.01	
+ 1 mM halothane	0.27	0.30 ± 0.02	8 ± 3
+ 3 mM halothane	0.28	0.35 ± 0.01	18 ± 2
Low Ca	0.50	0.48 ± 0.01	
+ 1 mM halothane	0.47	0.48 ± 0.01	Stimulated
+ 3 mM halothane	0.58	0.55 ± 0.01	43 ± 4
Low Ca, PLB phosphorylated	0.45	0.40 ± 0.01	
+ 1 mM halothane	0.47	0.46 ± 0.02	28 ± 8
+ 3 mM halothane	0.51	0.51 ± 0.01	67 ± 5

The fraction of immobile Ca-ATPase aggregates (f_I) determined by fitting TPA decays of ERITC-CSR at 25°C in the presence of 0–3 mM halothane to the uniaxial and multiexponential ($f_I = A_\infty'/1-A_{\infty 0}$) models (see Materials and Methods) compared with the percent inhibition of the Ca-ATPase (data from Fig. 6). To facilitate fitting to the more complex uniaxial model, TPA decays from three experiments were averaged, and the averaged TPA decay was fit (see Karon and Thomas, 1993). For the multiexponential model, three individual TPA decays were fit, and the values in the table represent the average of three experiments ± SE. Low Ca levels are 50 nM (for TPA decays) and 150 nM (for activity experiments).

halothane on the mole fraction of slowly rotating species (f_3) and immobile species (f_I) determined by fitting the TPA decays according to the uniaxial model are also plotted in Fig. 8*B*. Halothane increased the values of f_I and decreased the values of f_3 (aggregated the Ca-ATPase) under all conditions measured except at low Ca and low (1 mM) halothane, in which f_3 increased and f_I decreased (indicating dissociation of Ca-ATPase aggregates). Halothane-induced activation of the enzyme was seen only under these same conditions (Fig.

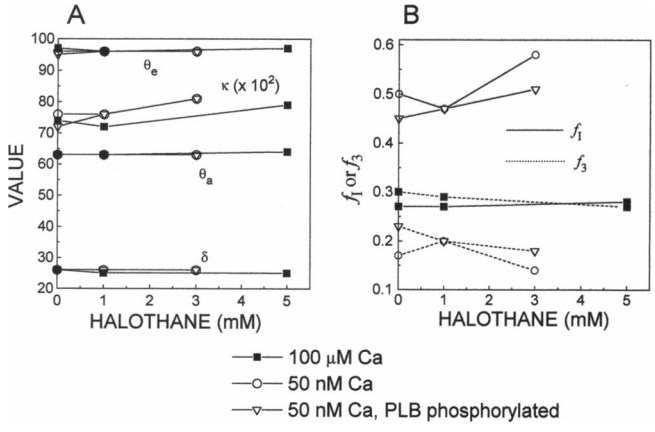

FIGURE 8 (*A*) The values of the probe dipole angles (relative to the membrane normal) θ_a, θ_e, and δ (see Materials and Methods), and the fast motion factor κ, determined by fitting to the uniaxial model (see Materials and Methods) TPA decays of ERITC-CSR at 25°C and 50 nM [Ca] (○), 50 nM [Ca] with PLB phosphorylated (▽), and 100 μM [Ca] (■), in the absence and presence of halothane. (*B*) The values of f_3 (mole fraction of slowly rotating Ca-ATPase oligomers) and f_I (mole fraction of immobile Ca-ATPase oligomers; see Table 1) determined by fitting TPA decays under the conditions described above.

5). Thus, the uniaxial model not only shows that halothane-induced aggregation of the Ca-ATPase correlates well with inhibition (Table 1) but also that halothane-induced activation of the Ca-ATPase (at low halothane and low Ca) correlates with dissociation into smaller oligomers. In skeletal SR, agents that aggregate the Ca-ATPase inhibit enzyme function, whereas agents that dissociate Ca-ATPase oligomers activate the enzyme (Mahaney and Thomas, 1991; Voss et al., 1991; Bigelow and Thomas, 1987; Birmachu and Thomas, 1990). For the case of halothane in CSR, this same relationship between Ca-ATPase oligomeric state and enzymatic function is seen, but halothane can either aggregate and inhibit (under most circumstances) or dissociate and activate (only at low Ca and low halothane concentrations) the enzyme.

DISCUSSION

Ca uptake versus ATPase activity in the presence of anesthetic agents

Anesthetic agents may affect in vitro measures of Ca regulation in SR by at least three independent mechanisms: (1) inhibition or activation of the Ca-ATPase; (2) inhibition or activation of the Ca release channel; or (3) change in the rate of passive Ca leak from SR, which can affect both the rate of Ca uptake and ATP hydrolysis measured (Bigelow and Thomas, 1987; Frazer and Lynch, 1992; Karon and Thomas, 1993; Kutchai et al., 1994). Previous attempts to assess anesthetic action on the Ca-ATPase in SR have found that lidocaine inhibits Ca-ATPase function in CSR, whereas halothane has been found to either activate or inhibit enzymatic activity (Lain et al., 1968; Katz et al., 1975; Casella et al., 1987; Frazer and Lynch, 1992). One study has found that halothane induces a passive leak of Ca from SR vesicles, which may explain conflicting results. The physiological relevance of this action is undetermined, as the halothane-induced passive leak probably does not occur in vivo (Frazer and Lynch, 1992). Furthermore, both halothane and lidocaine have been found to increase Ca-ATPase activity by inducing passive Ca leak in light skeletal SR, which lacks a substantial population of Ca release channels (Karon and Thomas, 1993; Kutchai et al., 1994). Moreover, halothane has been found to activate Ca release channels in both skeletal and cardiac SR (Frazer and Lynch, 1992; Louis et al., 1992).

Our study suggests that the effects of anesthetics on Ca uptake in CSR depend largely on the physiological state of the Ca release channel. When the channel is not inhibited, anesthetic-induced passive leak from SR vesicles is not likely to influence the apparent rate of Ca uptake, as the SR is already quite leaky to Ca via the release channel. In the presence of ruthenium red, lidocaine may first increase the rate of passive Ca leak, which results in an apparent decrease in the rate of Ca uptake. Higher concentrations of lidocaine decrease the rate of Ca uptake by inhibiting the Ca-ATPase (Fig. 1). Thus, the most interpretable in vitro indicator of anesthetic effects on Ca-ATPase function is Ca-ATPase activity in the presence of ionophore, rather than Ca uptake measurements. For this reason, Ca-ATPase activity in the presence of ionophore was used to detect anesthetic-induced changes in Ca-ATPase function in this study.

Lidocaine effects on Ca-ATPase activity and oligomeric state

It has previously been shown that lidocaine and other local anesthetics inhibit the Ca-ATPase in CSR and that this inhibition is competitive with respect to Ca (Katz et al., 1975). We found that lidocaine inhibited the Ca-ATPase in CSR, and this inhibition did not change the apparent K_m of the enzyme for Ca (Fig. 2). However, concentrations of Ca greater than necessary to saturate the high affinity Ca binding site did protect the enzyme from lidocaine-induced inhibition (Fig. 3). To further define this effect, we added 0.5 M LiCl in the presence of 20 μM [Ca] and found no inhibition of Ca-ATPase activity by 0–30 mM lidocaine. In addition, we added up to 1 mM (as much as is soluble in water) benzocaine to SR to determine whether this uncharged local anesthetic would inhibit Ca-ATPase activity. Although the concentration of benzocaine added was much less than the concentration of lidocaine used, the buffer:lipid partition coefficient of benzocaine is at least twice as great as that for lidocaine (Strichartz et al., 1990), so membrane concentrations of benzocaine were comparable with those used for lidocaine. No inhibitory effects of benzocaine were observed. We conclude that cationic charge is essential to the inhibitory mechanism of lidocaine. This suggests that lidocaine interacts with anionic sites in the cytoplasmic domain of the Ca-ATPase to inhibit the enzyme.

We have found that lidocaine aggregates the Ca-ATPase in CSR (Fig. 4). In contrast to the protective effect of Ca on lidocaine-induced inhibition, lidocaine-induced aggregation of the Ca-ATPase showed no clear dependence on [Ca] (Fig. 5). Addition of 0.5 M LiCl at 100 μM [Ca] did not abolish the Ca-ATPase aggregation induced by 0–5 mM lidocaine. In contrast, lidocaine-induced inhibition (from 0 to 30 mM lidocaine) was prevented by addition of 0.5 M LiCl at 20 μM [Ca] (Fig. 3). It is believed that the charged and uncharged lidocaine species play separate roles in inhibition of Na channels (Bokesch et al., 1986; Wendt et al., 1993). Similarly, lidocaine-induced aggregation of the Ca-ATPase could involve separate interactions of the hydrophobic and hydrophilic domains of lidocaine or of the uncharged (hydrophobic) and charged (hydrophilic) species. Nevertheless, it is clear that lidocaine-induced inhibition is dominated by cationic interaction with a hydrophilic (cytoplasmic) domain of the Ca-ATPase.

Comparison of lidocaine effects in skeletal and cardiac SR

Lidocaine has previously been shown to inhibit and aggregate the Ca-ATPase in skeletal SR (Kutchai et al., 1994). In skeletal SR at 20 μM [Ca], approximately 75 mM lidocaine

is needed to inhibit Ca-ATPase activity by one half (Kutchai et al., 1994). In CSR at 20 μM [Ca], approximately 30 mM lidocaine is needed to inhibit Ca-ATPase activity by one half (Fig. 3). The concentration of lidocaine necessary to produce detectable changes in the residual anisotropy of ERITC-skeletal SR at 100 μM [Ca] is 8.5 mM (Kutchai et al., 1994). The residual anisotropy of ERITC-CSR at 100 μM [Ca] is increased by lidocaine concentrations as low as 1 mM (Fig. 4). Thus, lidocaine inhibits and aggregates the Ca-ATPase in CSR at lower concentrations than required in skeletal SR. This could be due to (1) the presence of PLB in CSR; (2) a differential effect of lidocaine on SR lipids in cardiac as opposed to skeletal SR; or (3) a differential affinity for lidocaine between the cardiac and skeletal isoforms of the enzyme. The lipid environments of skeletal and cardiac SR are nearly identical (Birmachu et al., 1993), and we have determined that PLB Ab did not change the extent of Ca-ATPase inhibition by lidocaine. Thus, our results suggest that the cardiac isoform of the Ca-ATPase has a higher affinity for lidocaine than the skeletal isoform.

It has recently been shown that polyamines, such as spermine and spermidine, inhibit the Ca-ATPase in skeletal SR at millimolar concentrations (Hughes et al., 1994). These authors concluded that polyamines bound predominantly to an anionic site on the cytoplasmic domain of the skeletal isoform and that this may represent a site of PLB interaction with the cardiac isoform of the Ca-ATPase (Hughes et al., 1994). Our finding that lidocaine inhibition and aggregation occur with higher affinity in cardiac rather than skeletal SR suggest that a cytoplasmic domain on the cardiac isoform of the enzyme is more sensitive to the action of cationic compounds. Local anesthetics similar to lidocaine have been shown to interact with SR near the headgroup of the lipids or at the lipid-protein interface (Anteneodo et al., 1994; Louro et al., 1994). Thus, lidocaine may interact with anionic residues in the stalk domain of the Ca-ATPase, which are predicted to be near the membrane surface (Brandl et al., 1986). However, the action of lidocaine was not dependent on the regulatory state of PLB (presence of Ab). Thus, we cannot conclude that an anionic site in the stalk domain of the Ca-ATPase is the site of interaction for both PLB and lidocaine. Rather, the anionic residues in the stalk domain may interact with lidocaine and facilitate PLB-induced inhibition and aggregation of the Ca-ATPase.

Effects of halothane on Ca-ATPase activity and oligomeric state

We have found that halothane inhibits the Ca-ATPase in CSR and that both high Ca concentration and PLB interaction with the Ca-ATPase (which occurs at low Ca concentration in the absence of PLB phosphorylation or PLB Ab) protect against this inhibition (Fig. 6). This is in agreement with a previous study that found that halothane inhibition of the Ca-ATPase in CSR was competitive with respect to Ca (Malinconico and McCarl, 1982).

The nonionic detergent $C_{12}E_8$ also activates the Ca-ATPase in CSR only at low [Ca]. At high [Ca] or when PLB is phosphorylated, $C_{12}E_8$ inhibits the Ca-ATPase (Lu and Kirchberger, 1994). These authors concluded that $C_{12}E_8$ may physically dissociate PLB from the Ca-ATPase, resulting in enzymatic activation at low Ca (Lu and Kirchberger, 1994). It is possible that low levels of halothane might also dissociate PLB from the Ca-ATPase, activating the enzyme; whereas higher levels of halothane might act directly on the Ca-ATPase to inhibit enzymatic activity. More investigation is needed to define the mechanism of PLB and Ca protection against halothane-induced inhibition of the Ca-ATPase. It has also been reported that halothane inhibition of Ca uptake in CSR is dependent upon the concentration of ATP present (Blanck and Thompson, 1981). We found no effect of [ATP] on halothane-induced inhibition of Ca-ATPase activity. Because ATP has also been shown to activate the Ca release channel in skeletal SR (Mickelson et al., 1989), it is possible that Ca release rates were modified by ATP, resulting in changes in the rate of Ca uptake measured.

Halothane aggregates the Ca-ATPase in CSR (Fig. 7), and this aggregation correlates well with halothane-induced inhibition of the enzyme (Table 1). This suggests that halothane-induced aggregation of the Ca-ATPase plays a role in the mechanism of halothane-induced inhibition. We have fit the TPA decays of ERITC-CSR according to two models and found that the fraction of immobile aggregates calculated (f_i; Eq. 6) by the simple multiexponential model (Eqs. 2–4 and 6) agrees well with the fraction of immobile aggregates determined by fitting the decays to the analytical function that describes uniaxial diffusion of a membrane protein (Eqs. 5 and 7–10 and Table 1). Halothane increased the rapid submicrosecond motion of the ERITC probe but did not affect the angles between the membrane normal and the probe's absorption and emission dipoles (Fig. 8*A*). Because halothane does not change these probe angles, the value of $A_{\infty 0}$ will remain constant with halothane addition (Eqs. 3 and 4), so that halothane-induced increases in A_∞' must be due to an increased mole fraction of immobile Ca-ATPase aggregates. As was demonstrated for TPA decays of ERITC-skeletal SR (Cornea and Thomas, 1994; Mersol et al., 1995), the simple multiexponential model can be used to fit TPA decays and determine the mole fraction of immobile Ca-ATPase aggregates in CSR.

Comparison of halothane effects in skeletal and cardiac SR

We have previously observed that halothane activates and dissociates Ca-ATPase oligomers in skeletal SR (Karon and Thomas, 1993). In CSR, halothane inhibits and aggregates the Ca-ATPase. Halothane inhibition and aggregation are Ca-dependent in CSR, whereas we did not observe Ca dependence of halothane action in skeletal SR (data not shown). The opposite effects of halothane in skeletal SR and CSR could be due to the presence of PLB in CSR, as halothane effects in CSR are dependent upon the regulatory

state of PLB. However, phosphorylation of PLB (or PLB Ab) accentuated differences between skeletal SR and CSR (i.e., inhibition and aggregation were greater). Therefore, differential effects of halothane between skeletal SR and CSR must be due to either (1) PLB effects that occur exclusively under conditions (high [Ca] or PLB phosphorylation) that do not allow PLB regulation of the Ca-ATPase, or (2) halothane must interact with the cardiac isoform of the Ca-ATPase in a manner distinct from the skeletal isoform. More investigation is needed to determine the roles of PLB and the cardiac isoform of the Ca-ATPase in anesthetic perturbation of SR function.

General anesthetics (e.g., halothane) are known to depress myocardial contractility at clinical levels, and this may be due to a perturbation of SR Ca regulation (Rusy and Komai, 1987). Halothane activates Ca release in both skeletal SR and CSR (Frazer and Lynch, 1992; Louis et al., 1992), but halothane alters intracellular Ca levels only in cardiac muscle (Rusy and Komai, 1987; Iaizzo et al., 1988). A differential effect of halothane between skeletal SR and CSR could help explain anesthetic depression of myocardial contractility via SR Ca regulation. We find that halothane has opposite effects on the Ca-ATPase in skeletal SR and CSR. Halothane is also known to sensitize the heart towards arrhythmias induced by administration of β-adrenergics (Price and Ohnishi, 1980). As PLB is the predominant protein phosphorylated in SR after β-adrenergic stimulation (Lindermann et al., 1983), and phosphorylation of PLB sensitizes the Ca-ATPase to inhibition by halothane, a sudden reduction in the rate of Ca uptake may occur after β-adrenergic stimulation in the presence of halothane.

CONCLUSIONS

Lidocaine, a cationic local anesthetic, and halothane, a hydrophobic general anesthetic, have different functional effects in cardiac SR, and these anesthetic effects are different from those in skeletal SR. Both of these differences can be explained to a remarkable extent by a single physical model: Aggregation inhibits the Ca-ATPase. Lidocaine inhibits and aggregates the Ca-ATPase in cardiac SR, with both effects occuring at lower levels than in skeletal SR. Lidocaine's effects are primarily due to electrostatic interactions with an anionic site on the cytoplasmic domain of the Ca-ATPase, and this site may facilitate PLB-induced Ca-ATPase aggregation. Halothane inhibits and aggregates the Ca-ATPase in cardiac SR under most conditions, opposite its effects in skeletal SR. PLB phosphorylation, which is thought to uncouple PLB from the Ca-ATPase, increases the inhibitory effect of halothane, indicating that the opposite effects of halothane in cardiac and skeletal SR are not easily explained by the presence of PLB in cardiac SR. The mechanism of halothane-induced inhibition of the Ca-ATPase in cardiac SR involves formation of large Ca-ATPase oligomers.

We thank Dr. Joseph J. Feher, Medical College of Virginia, for the generous gift of CSR. We are also pleased to thank Dr. Larry Jones, Indiana University School of Medicine, for the anti-PLB Ab 2D12. We also thank James Mahaney, Razvan Cornea, and Joe Mersol for their help and Nicoleta Cornea, John Matta, and Bob Bennett for technical support.

D. D. T. was supported by National Institutes of Health (NIH) Grant GM27906. H. K. was supported by Grant-in-Aid VA-93-G-20 from the American Heart Association, Virginia, and NIH Grant GM50764. B. S. K. was supported in part by a NIH predoctoral training grant.

REFERENCES

Anteneodo, C., A. M. Rodahl, E. Meiering, M. L. Heynen, G. A. Sennisterra, and J. R. Lepock. 1994. Interaction of dibucaine with the transmembrane domain of the Ca-ATPase of sarcoplasmic reticulum. *Biochemistry.* 33: 12283–12290.

Bevington, P. R. 1969. Data Reduction and Error Analysis for the Physical Sciences. McGraw-Hill, New York.

Bigelow, D. J., and D. D. Thomas. 1987. Rotational dynamics of lipid and the Ca-ATPase of sarcoplasmic reticulum. *J. Biol. Chem.* 262: 13449–13456.

Birmachu, W., F. L. Nisswandt, and D. D. Thomas. 1989. Conformational transitions in the Ca-ATPase studied by time-resolved fluorescence energy transfer. *Biochemistry.* 28:3940–3947.

Birmachu, W., and D. D. Thomas. 1990. Rotational dynamics of the Ca-ATPAse in sarcoplasmic reticulum studied by time-resolved phosphorescence anisotropy. *Biochemistry.* 29:3904–3914.

Birmachu, W., J. C. Voss, C. F. Louis, and D. D. Thomas. 1993. Protein and lipid dynamics in cardiac and skeletal sarcoplasmic reticulum detected by EPR and phosphorescence anisotropy. *Biochemistry.* 32:9445–9453.

Blanck, T. J. J., and M. Thompson. 1981. Calcium transport by cardiac sarcoplasmic reticulum: modification of halothane action by substrate concentration and pH. *Anesth. Analg.* 60:390–394.

Bokesch, P. M., C. Post, and G. Strichartz, G. 1986. Structure-activity relationship of lidocaine homologs producing tonic and frequency-dependent impulse blockade in nerve. *J. Pharmacol. Exp. Ther.* 237:773–781.

Brandl, C. J., N. M. Green, B. Korczak, and D. H. MacLennan. 1986. Two Ca-ATPase genes: homologies and mechanistic implications of deduced amino acid sequences. *Cell.* 44:597–607.

Cantilina, T., Y. Sagara, G. Inesi, and L. R. Jones. 1993. Comparative studies of cardiac and skeletal sarcoplasmic reticulum ATPases. *J. Biol. Chem.* 268:17018–17025.

Casella, E. S., N. D. A. Suite, Y. I. Fisher, and T. J. J. Blanck. 1987. The effect of volatile anesthetics on the pH dependence of calcium uptake by cardiac sarcoplasmic reticulum. *Anesthesiology.* 67:386–390.

Cornea, R. L., and D. D. Thomas. 1994. Effects of membrane thickness on the molecular dynamics and enzymatic activity of reconstituted Ca-ATPase. *Biochemistry.* 33:2912–2920.

Eads, T. M., D. D. Thomas, and R. H. Austin. 1984. Microsecond rotational motions of eosin-labeled myosin measured by time-resolved anisotropy absorption and phosphorescence. *J. Mol. Biol.* 179:55–81.

Feher, J. J., and F. N. Briggs. 1983. Determinants of calcium loading at steady state in sarcoplasmic reticulum. *Biochim. Biophys. Acta.* 727:389–402.

Franks, N. P., and W. R. Lieb. 1994. Molecular and cellular mechanisms of general anesthesia. *Nature.* 367:607–614.

Frazer, M. J., and C. Lynch. 1992. Halothane and isoflurane effects on Ca fluxes of isolated myocardial sarcoplasmic reticulum. *Anesthesiology.* 77:316–323.

Hughes, G., A. P. Starling, M. East, and A. G. Lee. 1994. Mechanism of inhibition of the Ca-ATPase by spermine and other polycationic compounds. *Biochemistry.* 33:4745–4754.

Iaizzo, P. A., W. Klein, and F. Lehmann-Horn. 1988. Fura-2 detected myoplasmic calcium and its correlation with contracture force in skeletal muscle from normal and malignant hyperthermia susceptible pigs. *Pflugers Arch.* 411:648–653.

James, P., M. Inui, M. Tada, M. Chiesi, and E. Carafoli. 1989. Nature and site of phospholamban regulation of the Ca pump of sarcoplasmic reticulum. *Nature.* 342:90–92.

Karon B. S., J. E. Mahaney, and D. D. Thomas. 1994. Halothane and cyclopizonic acid modulate Ca-ATPase oligomeric state and function in sarcoplasmic reticulum. *Biochemistry.* 33:13928–13937.

Karon, B. S., and D. D. Thomas. 1993. Molecular mechanism of Ca-ATPase activation by halothane in sarcoplasmic reticulum. *Biochemistry.* 32:7503–7511.

Katz, A. M., D. I. Repke, S. Corkedale, and J. Schwarz. 1975. Effects of local anesthetics on calcium transport by canine microsomes (fragmented sarcoplasmic reticulum). *Cardiovasc. Res.* 9:764–769.

Kinosita, K., S. Kawato, and A. Ikegami. 1977. A theory of fluorescence polarization decay in membranes. *Biophys. J.* 20:289–305.

Kutchai, H., and K. P. Campbell. 1989. Calcium transport by sarcoplasmic reticulum of skeletal muscle is inhibited by antibodies against the 53 kD glycoprotein of the sarcoplasmic reticulum membrane. *Biochemistry.* 28: 4830–4839.

Kutchai, H., J. E. Mahaney, L. M. Geddis, and D. D. Thomas. 1994. Hexanol and lidocaine affect the oligomeric state of the Ca-ATPase of sarcoplasmic reticulum. *Biochemistry.* 33:13208–13222.

Lain, R. F., M. L. Hess, E. W. Gertz, and F. N. Briggs. 1968. Calcium uptake activity of canine myocardial sarcoplasmic reticulum in the presence of anesthetic agents. *Circ. Res.* 23:597–604.

Lindemann, J. P., L. R. Jones, D. R. Hathaway, and B. G. Henry. 1983. β-adrenergic stimulation of phospholamban phosphorylation and Ca-ATPase activity in guinea pig ventricles. *J. Biol. Chem.* 258:464–471.

Lipari, G., and A. Szabo. 1980. Effect of librational motion on fluorescence depolarization and nuclear magnetic resonance relaxation in macromolecules and membranes. *Biophys. J.* 30:489–506.

Louis, C. F., K. Zualkernan, T. Roghair, and J. R. Mickelson. 1992. The effects of volatile anesthetics on calcium regulation by malignant hyperthermia-susceptible sarcoplasmic reticulum. *Anesthesiology.* 77:114–125.

Louro, S. R. W., M. Tabak, and O. R. Nascimento. 1994. Depth profiling of dibucaine in sarcoplasmic reticulum vesicles by fluorescence quenching. *Biochim. Biophys. Acta.* 1189:243–246.

Lu, Y., and M. A. Kirchberger. 1994. Effects of a nonionic detergent on calcium uptake by cardiac microsomes. *Biochemistry.* 33: 5056–5062.

Ludescher, R. D., and D. D. Thomas. 1988. Microsecond rotational dynamics of phosphorescent-labeled muscle cross-bridges. *Biochemistry.* 27:3343–3351.

Mahaney, J. E., and D. D. Thomas. 1991. Effects of melittin on molecular dynamics and Ca-ATPase activity in sarcoplasmic reticulum membranes: electron paramagnetic resonance. *Biochemistry.* 30:7171–7180.

Malinconico, S. M., and R. L. McCarl. 1982. Effect of halothane on cardiac sarcoplasmic reticulum Ca-ATPase at low calcium concentrations. *Mol. Pharmacol.* 22:8–10.

Mersol, J. V., H. Kutchai, J. E., Mahaney, and D. D. Thomas. 1995. Self-association accompanies inhibition of Ca-ATPase by thapsigargin. *Biophys. J.* In press.

Mickelson, J. R., E. M. Gallant, W. E. Rempel, K. M. Johnson, L. A. Litterer, B. A. Jacobson, and C. F. Louis. 1989. Effects of the halothane-sensitivity gene on sarcoplasmic reticulum function. *Am. J. Physiol.* 257:C787–C794.

Moutin, M., C. Rapin, and Y. Dupont. 1992. Ruthenium red affects the intrinsic fluorescence of the Ca-ATPase of skeletal muscle sarcoplasmic reticulum. *Biochim. Biophys. Acta.* 1100:321–328.

Price, H. L., and S. T. Ohnishi. 1980. Effects of anesthetics on the heart. *Fed. Proc.* 39:1575–1579.

Restall, C. J., R. E. Dale, E. K. Murray, C. W. Gilbert, and D. Chapman. 1984. Rotational diffusion of Ca-ATPase in sarcoplasmic reticulum: a detailed study. *Biochemistry.* 23:6765–6776.

Rusy, B. F., and H. Komai. 1987. Anesthetic depression of myocardial contractility: a review of possible mechanisms. *Anesthesiology.* 67:745–766.

Saffman, P. J., and M. Delbrück. 1975. Brownian motion in biological membranes. *Proc. Natl. Acad. Sci. USA.* 72:3111–3113.

Sasaki, T., M. Inui, T. Kimura, M. Tada. 1992. Molecular mechanism of regulation of Ca pump ATPase by phospholamban in cardiac sarcoplasmic reticulum. *J. Biol. Chem.* 267:1674–1679.

Sham, J. S. K., L. R. Jones, and M. Morad. 1991. Phospholamban mediates the β-adrenergic-enhanced Ca uptake in mammalian ventricular myocytes. *Am. J. Physiol.* 261:H1344–H1349.

Squier, T. C., D. J. Bigelow, and D. D. Thomas. 1988a. Lipid fluidity directly modulates the overall rotational mobility of the Ca-ATPase in sarcoplasmic reticulum. *J. Biol. Chem.* 263:9178–9186.

Squier, T. C., S. E. Hughes, and D. D. Thomas. 1988b. Rotational dynamics and protein-protein interactions in the Ca-ATPase mechanism. *J. Biol. Chem.* 263:9162–9170.

Squier T. C., and D. D. Thomas. 1989. Selective detection of the rotational dynamics of the protein-associated lipid hydrocarbon chains in sarcoplasmic reticulum membranes. *Biophys. J.* 56:735–748.

Strichartz, G. R., V. Sanchez, R. Arthur, R. Chafetz, and D. Martin. 1990. Fundamental properties of local anesthetics. *Anesth. Analg.* 71:158–170.

Szabo, A. 1984. Theory of fluorescence depolarization in macromolecules and membranes. *J. Chem. Phys.* 81:150.

Thomas, D. D., and B. S. Karon. 1994. Temperature dependence of molecular dynamics and calcium ATPase activity in sarcoplasmic reticulum. *In* The Temperature Adaptation of Biological Membranes. A. R. Cossins, editor. Portland Press, London. 1–12.

Voss, J., D. Hussey, W. Birmachu, and D. D. Thomas. 1991. Effects of melittin on molecular dynamics and Ca-ATPase activity in sarcoplasmic reticulum membranes: time-resolved optical anisotropy study. *Biochemistry.* 30:7498–7506.

Voss, J., L. R. Jones, and D. D. Thomas. 1994. The physical mechanism of calcium pump regulation in the heart. *Biophys. J.* 67:190–196.

Wendt, D. J., C. F. Starmer, and A. O. Grant. 1993. pH dependence of kinetics and steady-state block of cardiac sodium channels by lidocaine. *Am. J. Physiol.* 264:H1588–H1598.